Tim S. Böscke (Autor)

Crystalline Hafnia and Zirconia based Dielectrics for Memory Applications

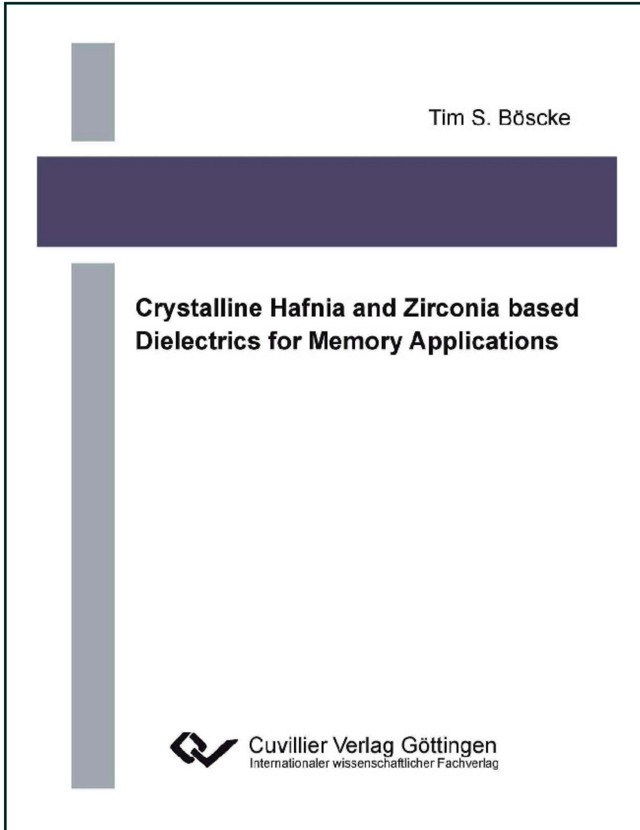

https://cuvillier.de/de/shop/publications/763

Copyright:
Cuvillier Verlag, Inhaberin Annette Jentzsch-Cuvillier, Nonnenstieg 8, 37075 Göttingen, Germany
Telefon: +49 (0)551 54724-0, E-Mail: info@cuvillier.de, Website: https://cuvillier.de

Chapter 1

Introduction

Progress in scaling of integrated circuits requires continued innovation in many areas. In the past few years, the reduction of the electrical thickness of gate- and capacitor insulators became one of the most challenging topics. While this was previously achieved by simple reduction of the physical thickness of the ubiquitous silicon oxide/silicon nitride based dielectric, increasing leakage currents prevented scaling into the sub nanometer regime. Further improvements are only possible by introducing materials with a higher permittivity, so called high-k dielectric, to allow a reduction of electrical thickness without decreasing physical thickness.

The leading candidates for high-k dielectrics in gate insulators and dynamic random access memory (DRAM) capacitors are currently hafnium and zirconium based oxides. The initial motivation for this thesis was to understand their application to deep trench DRAM capacitors to enable capacitors for a sub 50 nm node, requiring a capacitance equivalent thickness (CET) below 3 nm [1]. As shown in table 1.1, this can not be achieved with medium-k dielectric like silicon oxynitride or aluminum oxide (Al_2O_3) and requires the introduction of hafnium silicon oxide (HfSiO) and metal electrodes.

A central theme of material engineering of HfO_2 and ZrO_2 for microelectronic applications has been to control the degree of crystallinity during deposition and subsequential thermal annealing steps [2]. This was motivated by a multitude of

Node	90 nm	70 nm	60 nm	50 nm	40 nm
CET	5.0 nm	4.0 nm	3.5 nm	2.5 nm	1.8 nm
	SIS SiON	SIS SiON	MIS Al_2O_3	MIS HfSiO	MIM HfSiO

Table 1.1: Deep trench DRAM capacitor CET requirements according to [1]. SIS=Silicon Insulator Silicon, MIS=Metal Insulator Silicon, MIM=Metal Insulator Metal.

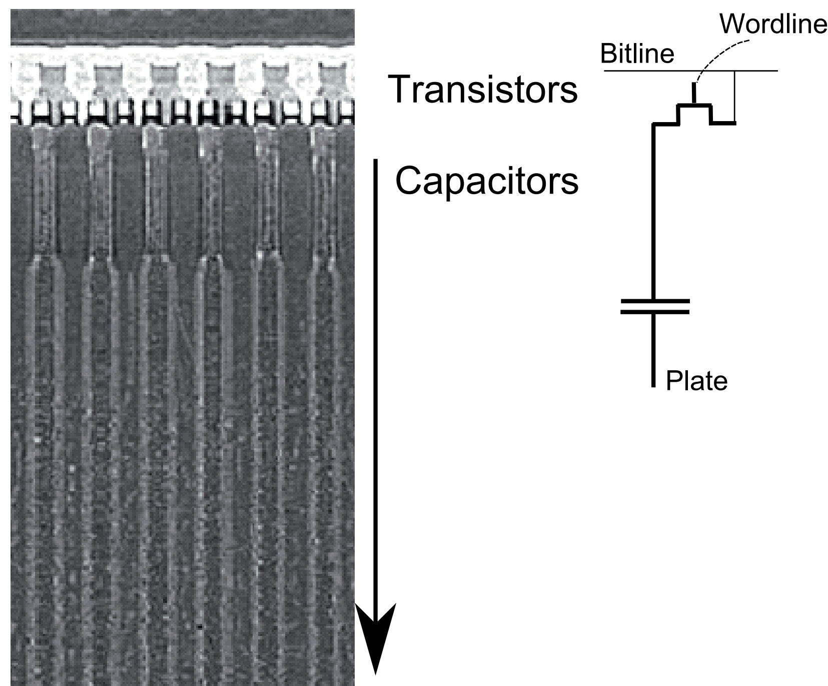

Figure 1.1: Cross section of a deep trench DRAM array (90 nm technology) and equivalent circuit of a single cell.

issues with the crystalline form, such as: Diffusion of dopants at grain boundaries [3], mechanical defects during crystallization [4] and charge traps associated with the crystalline phase [5, 6]. Two common approaches to preventing crystallization are reducing the thermal budget, as applied in stack capacitor DRAM [7], or reducing the film thickness, as applied in transistors [8].

Dielectrics for deep trench DRAM capacitors [9] have to withstand a high thermal budget above 1000°C because the capacitor is processed before access transistor formation (See cross section in figure 1.1). At the same time, a relatively thick dielectric is required to meet the leakage current specification of 10^{-7}A/cm^2 or less at 1 V. Since thicker films crystallize more easily [10], crystallization of a hafnium rich dielectric can not be prevented in this case. The key challenge for the application of HfO_2 and ZrO_2 in deep trench DRAM is therefore to understand and engineer the *crystalline* state.

While the crystalline state poses additional difficulties in regard to defect engineering, it also offers the opportunity to optimize crystalline phases in respect to dielectric constants. Simulations show that both HfO_2 and ZrO_2 can exhibit dielectric constants between 18 and 36, depending on crystalline phase. Controlled manipulation of the phase composition does therefore allow to maximize

Crystalline phase	HfO_2	ZrO_2
amorphous	21	23
monoclinic	16-18	20
cubic	26.2	33.6
tetragonal	28.5	38.9

Table 1.2: Simulation results for the dielectric constants of the normal pressure HfO_2 and ZrO_2 phases [13, 14, 15].

the dielectric constant above that of the amorphous phase. Results published by other groups [11, 12] during the initial phase of this work confirmed this concept and encouraged pursuing phase stabilization to maximize dielectric constants.

1.1 Organization of Thesis

Although the motivation for this thesis emerged from a specific application, the results of this work can be applied in a much broader context. For example, similar material engineering challenges can be found in the application of thick HfSiO layers in flash memory. Furthermore, the discovery of ferroelectricity in HfSiO, as outlined later, enables application of HfSiO in a novel nonvolatile memory scheme.

Instead of following an application driven top down approach, the results are presented in a form that enables general understanding of the crystallography of ZrO/HfO thin films and the impact on dielectric properties. The specific application for DRAM capacitors is then derived from these results.

A general literature review of previous work on crystalline HfO_2 and ZrO_2 will be given in chapter 2. Emphasis is put especially on work in ceramics research which is relevant for microelectronic application. Chapter 3 outlines the experimental techniques used in this work.

The experimental results are reported in chapters 4-9 and are ordered with increasing system complexity. First, the ZrO_2 system, which is only represented in a single crystalline modification in nanoscale thin films, is investigated in chapter 4. The next chapter deals with HfO_2, which tends to occur as a mixture between two crystalline phases in thin films. Chapter 6 studies doping of SiO_2 into HfO_2, allowing controlled phase manipulation. The chapter concludes with an investigation of the electronic properties of HfSiO capacitors. Chapter 7 reports the effect of mechanical confinement on the crystallization of HfSiO, which allows to manipulate the dielectric properties of this material. Chapter 8 is dedicated to a detailed exploration of the physical and electronic properties of capped HfSiO,

revealing ferroelectric and antiferroelectric behavior. These findings enable the construction of a nonvolatile memory device, the ferroelectric field effect transistor, which is investigated in chapter 9. Chapter 10 concludes the thesis with a summary.

Chapter 2

Crystallography of ZrO_2/HfO_2

Even though the application of zirconium and hafnium oxide as electronic material is relatively new, both materials are widely used as bulk ceramics. Of special interest is the discovery of transformation toughening of zirconia in the mid 1970s [16, 17], ”Ceramic Steel”. Here, the volume expansion during the transformation of a metastable tetragonal phase into the monoclinic phase is used to slow crack propagation and allow significant improvement in fracture toughness. This finding stimulated research into the crystallography of doped zirconia and, to a lesser extend, hafnia.

Apart from a few notable exceptions, input from ceramics research has not been widely utilized by the semiconductor community. One of the reasons is that the initial objective of work on ZrO_2/HfO_2 was to find an amorphous replacement for SiO_2 gate dielelectrics [2]. However, moving toward application of crystalline films for DRAM, understanding of the crystallography of thin films becomes a necessity. This section provides a short literature review and will serve as reference for the experimental work in this thesis.

For the application of these materials in thin films, especially the influence of the specific surface area on phase stability is of relevance. This has been researched comprehensively in powders and will be discussed later in this chapter.

2.1 Undoped Oxides

Generally, it is important to realize that zirconium and hafnium oxide are chemically almost identical [18]. Both metals have similar ionic radii[1] which implies that also their crystal chemistry is very similar. A consequence of this similarity is that both oxides are fully miscible. The main differences are enthalpies of formation and free energy of the crystal surfaces, leading to deviations in phase

[1] 83 pm and 84 pm for eightfold coordinated Hf^{4+} and Zr^{4+} respectively [19].

transformation temperatures and phase stability for small crystallites with high surface area.

2.1.1 Normal Pressure Phases

At ambient pressure, both ZrO_2 and HfO_2 exhibit three different polymorphs (Figure 2.1): monoclinic, tetragonal, and cubic. Transformations between these phases take place depending on temperature [20]:

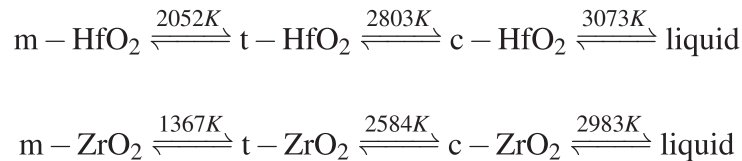

$$\mathrm{m-HfO_2} \xrightleftharpoons{2052K} \mathrm{t-HfO_2} \xrightleftharpoons{2803K} \mathrm{c-HfO_2} \xrightleftharpoons{3073K} \mathrm{liquid}$$

$$\mathrm{m-ZrO_2} \xrightleftharpoons{1367K} \mathrm{t-ZrO_2} \xrightleftharpoons{2584K} \mathrm{c-ZrO_2} \xrightleftharpoons{2983K} \mathrm{liquid}$$

The stability of these phases is defined in competition of entropy and enthalpy. The higher temperature phases become more and more symmetric and are therefore entropically more stable. However, the formation of higher symmetry phases in ZrO/HfO requires the reduction of the metal-oxygen bond distance, which leads to a chemically less desirable structure. Generally, a phase transformation can take place if the Gibbs free energy difference between two phases, a and b, approaches zero:

$$\Delta G_{a\rightarrow b} = 0 = \Delta H_{a\rightarrow b} - T\Delta S_{a\rightarrow b} \tag{2.1}$$

Here $\Delta H_{a\rightarrow b}$ is the enthalpy difference, T the temperature, and $\Delta S_{a\rightarrow b}$ the change of entropy. Rearranging yields the phase transition temperature $T_{a\rightarrow b}$:

$$T_{a\rightarrow b} = \frac{H_{a\rightarrow b}}{S_{a\rightarrow b}} \tag{2.2}$$

The first order tetragonal to monoclinic phase transformation is of special relevance, as significant structural changes occur in the crystal: The unit cell increases by 4-5% in volume and shears by approximately 9°. The cation coordination reduces from 8 to 7 which allows elongation of the metal oxygen bond to an energetically preferred configuration. The transformation is known to exhibit a hysteretic behavior which indicates an energy barrier between the two phases and gives rise to the existence of metastable phases. The exact nature of this phase transformation is not completely understood yet, but it is believed to involve an intermediate orthorhombic phase [21, 22]. Structural changes during the tetragonal to monoclinic transformation cause large mechanical stress which can be unloaded by microcracking [23], potentially leading to physical damage of the polycrystal.

The tetragonal to cubic phase transformation is not accompanied by a volume change and is suggested to be of second order [24]. The main difference between

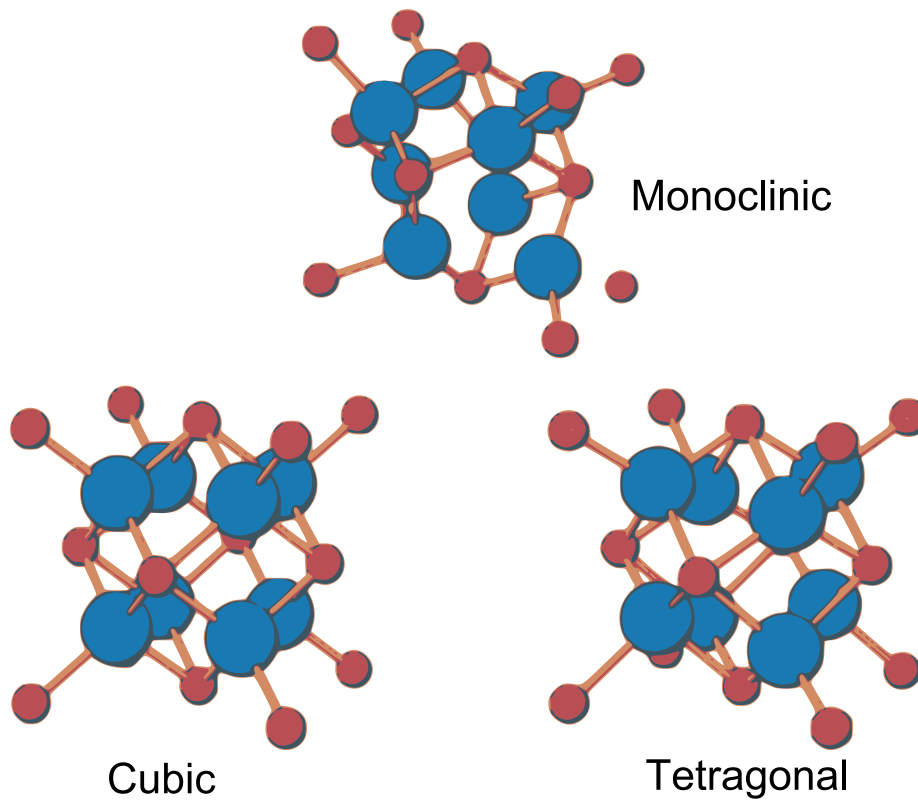

Figure 2.1: Normal pressure phases of hafnium and zirconium oxide (Reproduced from [23]).

these phases is a displacement of oxygen atoms along one axis of the tetragonal phase which leads to an expansion of the unit cell along the c axis. During the transition to the cubic phase, this displacement disappears gradually, decreasing Me-O bond lengths and increasing symmetry.

2.1.2 High Pressure Phases

When pure ZrO_2 is subjected to high pressure, it adopts one of two orthorhombic structures; between 3.5 and 15 GPa a phase with *Pbca* space group is formed while for higher pressure the cotunnite phase (*Pnam*) is observed. (see figure 2.2). The *Pbca* phase was experimentally also found for HfO_2, although at a slightly higher pressure of 4.2 GPa [25] or 6 GPa [26]. It appears likely that the cotunnite phase exists for HfO_2 as well, however no experimental evidence has been reported so far.

The occurrence of one of these phases in thin films appears unlikely due to the requirement of high compressive stress - most deposition techniques lead to tensile

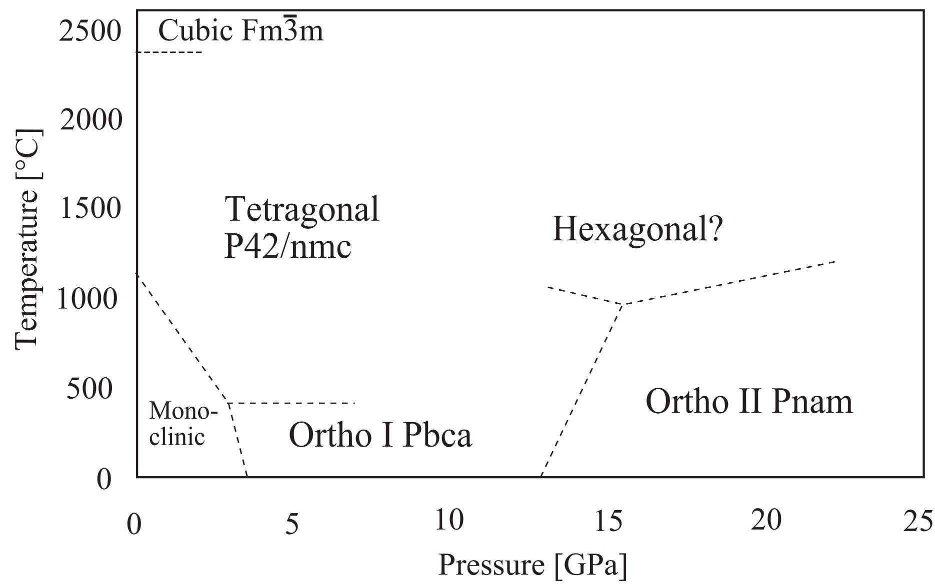

Figure 2.2: Temperature-Pressure phase diagram of zirconium oxide (Reproduced from [24]).

stress caused by volume reduction during subsequent crystallization. Nevertheless, several researchers report observation of the *Pbca* phase in thin films of HfO_2 [27]. Possible sources of misinterpretation could be formation of the *Pbca* phase during TEM sample preparation [24] or ambiguities in diffraction data interpretation [26].

2.2 Phase Stabilization

In ceramics terms, phase stabilization refers to the addition of suitable metal oxides (dopants) to stabilize a desired phase that would not be stable in the pure material. In the HfO_2/ZrO_2 system this does usually imply stabilization of the tetragonal or the cubic phase at normal pressure and low temperatures. Typical concentrations of dopants vary between 0 mol% and 20 mol%. The most common ceramic stabilizers are trivalent metals with atomic radii similar to Zr/Hf - essentially all rare earth elements. However, also group two elements like Ca, Mg, Ba are frequently used.

In contrast to ceramics research, semiconductor research has mainly focused on the addition of Al_2O_3 or SiO_2 with the primary goal of increasing the crystallization temperature and retaining an amorphous state during thermal processing steps.

2.2.1 Trivalent Dopants

Substitution of tetravalent zirconium or hafnium by trivalent ions leads to a charge imbalance in the crystal lattice. This is compensated by the formation of one oxygen vacancy for every two dopant atoms. The introduction of oxygen vacancies into a cubic lattice reduces the coordination number of adjacent cations to 7 and allows a shift of neighboring oxygen atoms to reduce *oxygen crowding* [28, 29, 30].

The efficiency of this mechanism is governed by the ionic radius ratio between the dopant and the host cation [31, 32]. The oxygen vacancy is not a direct neighbor of the dopant, if the dopant is larger than the host matrix cation. In that case, the dopant will retain a coordination number of 8 and a higher fraction of Hf/Zr atoms can adopt a coordination number of 7. This condition is satisfied by yttrium (101.9 pm for CN 8) which is the most common trivalent stabilizer.

Aluminum, which is a common dopant in high-k dielectric research, is too small to be effectively incorporated into the cubic lattice. Hence, the solubility in all HfO_2/ZrO_2 phases is relatively low, leading to segregation of Al_2O_3 to form a separate α or γ-alumina phase [33, 34]. However, although Al_2O_3 is not able to stabilize the cubic phase, it can stabilize the tetragonal phase by grain size reduction [35].

A simple model [36] predicts that 12.5 mol% of stabilizer has to be added to reduce the coordination number of all cations to 7. At this point the cubic phase is stabilized and transformation to the monoclinic phase is suppressed. Full stabilization is usually observed at even lower dopant concentrations, due to the additional entropic advantage of the tetragonal or cubic phase. Figure 2.3 shows an equilibrium phase diagram of thermodynamically stable regions.

2.2.2 Metastable Phases

For low dopant addition, the cubic phase can be stable at high temperature, but instable at room temperature (See position A in Fig. 2.3). During cooling, a separation into dopant rich cubic crystallites and tetragonal regions, which are depleted of dopants, takes place within the T+C stability region in the equilibrium phase diagram (Fig. 2.3, position B). The tetragonal fraction transforms to monoclinic upon further cooling (Pos. C). These phase separation processes involves the diffusion of cations and are, therefore, known as *diffusional* phase separation [38].

The diffusion of cations in ZrO_2 (and also HfO_2) is a relatively slow process

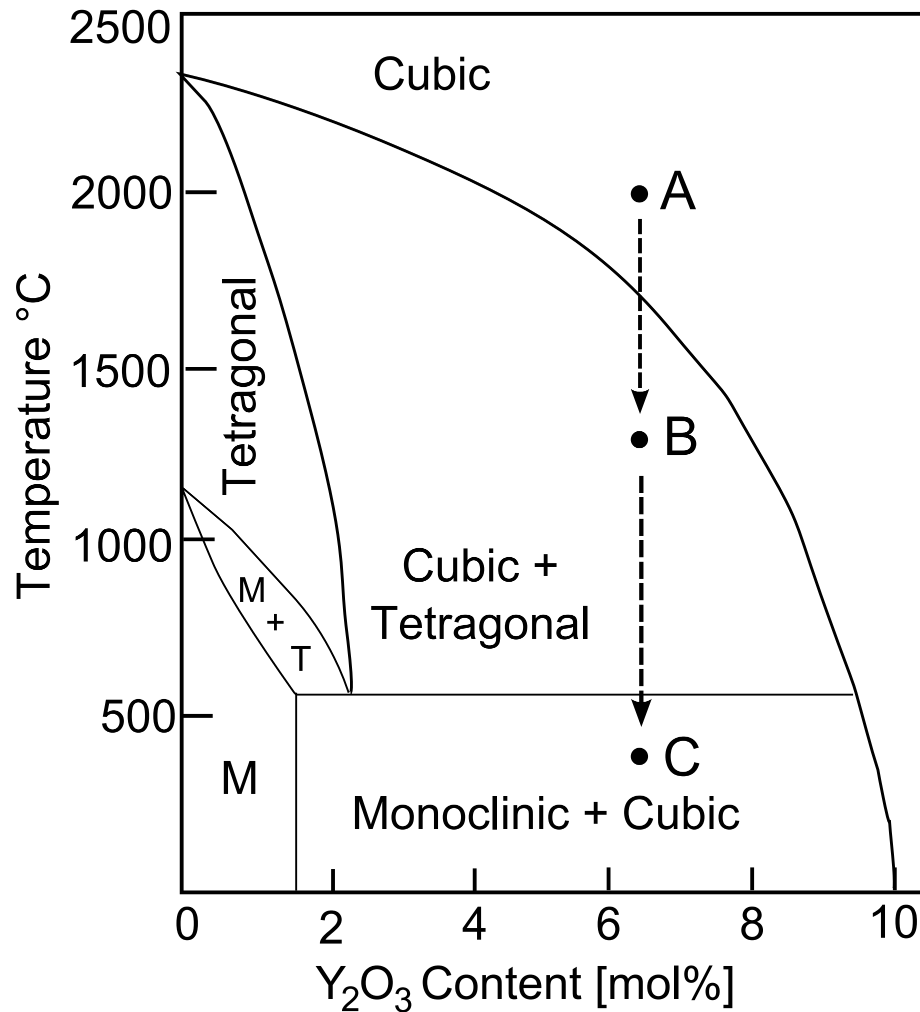

Figure 2.3: Phase diagram of the ZrO_2-Y_2O_3 system (Redrawn from [17]). The HfO_2-Y_2O_3 system is similar, mainly distinguished by the occurence of the monoclinic phase at higher temperature [37].

[38]. If very rapid cooling (quenching) from the cubic phase stability region or crystallization of an amorphous mixture occurs, a situation may arise where the phase separation process can not be completed before the cations are immobilized at low temperature. In this case, a *diffusionless* transformation into a single metastable phase takes place. This is of special relevance for applications within semiconductors technology, since most thermal processes take place at temperatures below 1000 °C and at relatively short timescales (seconds to hours).

Phases emerging during the diffusionless transformation are generally metastable, meaning that they do not represent the configuration with the lowest free energy and are prevented from reaching this state by the existence of an energy barrier (in this case a kinetic barrier involving cation diffusion). For trivalent dopants in ZrO_2 and HfO_2, the most relevant metastable phase is the tetragonal t' phase [39, 40, 41] with the same space group as the high temperature t phase ($P4_2/nmc$), but a lower c/a ratio ($1<c/a<1.028$). The c/a ratio of the t' phase reduces as the doping is increased until it approaches unity. At this point, a phase with cubic unit cell but displaced oxygen atoms is formed which is known as t" or c' (pseudocubic) phase [42, 39]. For higher doping, the oxygen displacement disappears and the cubic *Fm3m* phase is stable.

Diffusionless transformations into and between metastable phases are defined by the T_0 temperature at which the Gibbs free energy of both phases is equal without additional free energy lowering by separation into two or more phases. Using this concept, it is possible to design a metastable-stable phase diagram [38] as shown in figure 2.5.

A number of diffusionless phase transitions have been identified [43, 44] during cooling from the high temperature cubic phase. Initially, the cubic phase transforms into the t" phase by displacement of the oxygen sublattice. This phase will eventually transform into the t' phase. It has been shown that an energy barrier exists between the t' and the t" phase, based on the coexistence of these phases in the same sample. Corresponding to the t→m transformation a t'→m' transition occurs at lower temperatures.

An important parameter of the t' phase is its *transformability* into the monoclinic phase. The stability of the t' phase increases with decreased c/a ratio, increasing the transformation temperature T_0 and decreasing transformability due to mechanical stress [45]. As mentioned above, the c/a ratio of the metastable t' phase reduces with higher doping.

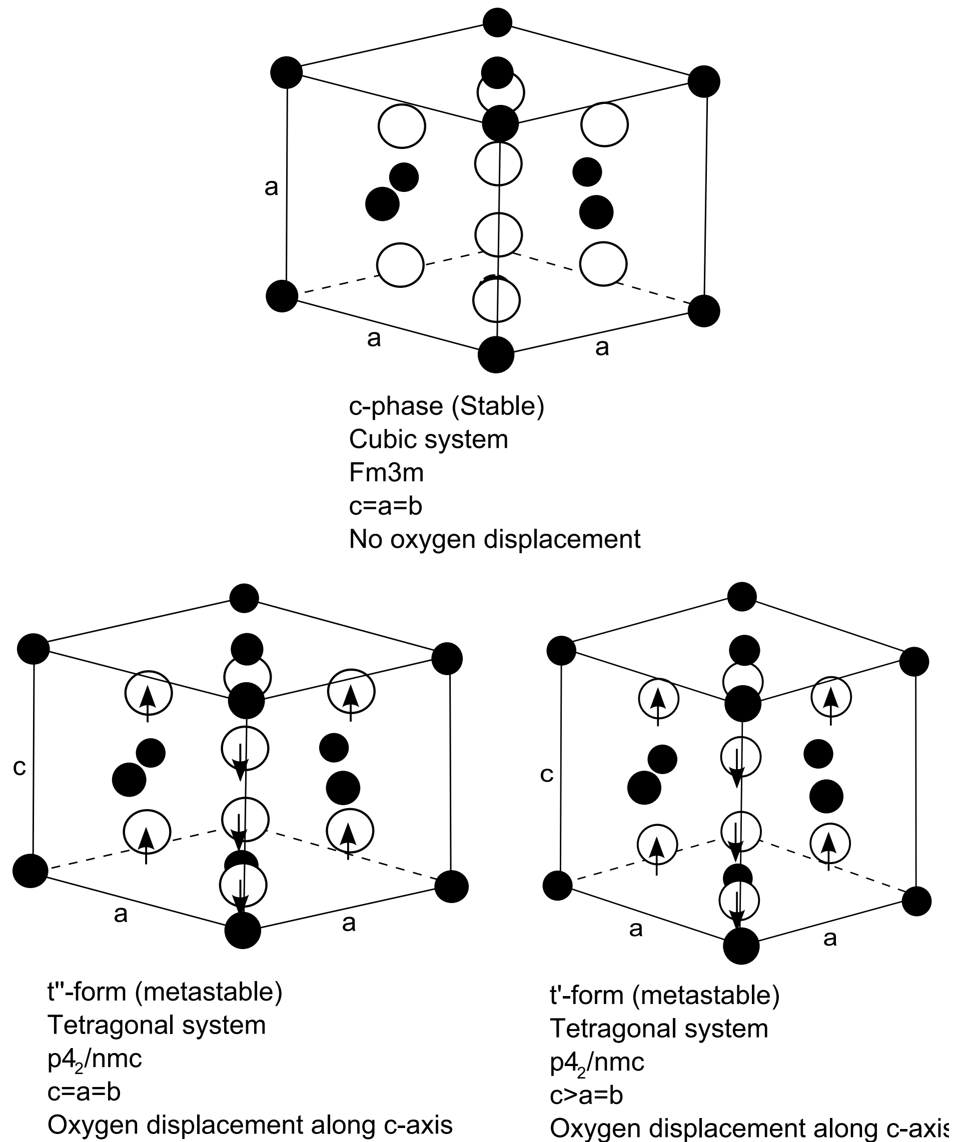

Figure 2.4: The metastable t' and t'' phases of ZrO_2 and HfO_2 (See [38]).

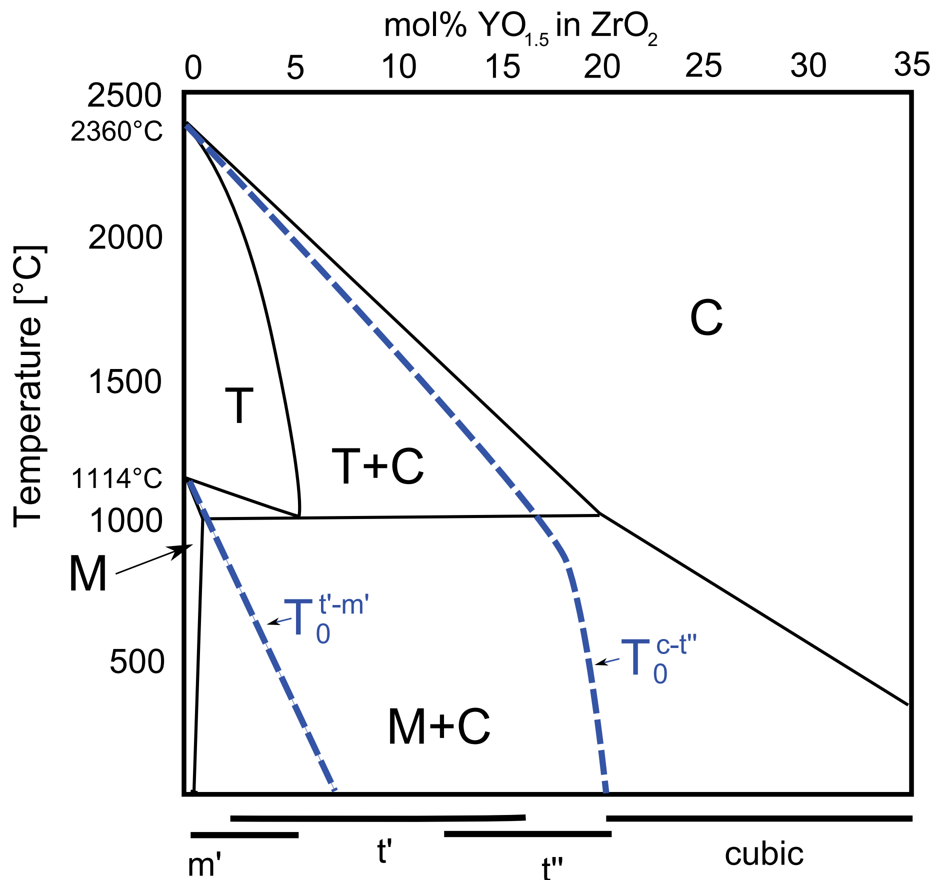

Figure 2.5: Equilibrium phase diagram of the ZrO_2-Y_2O_3 system with additional stability regions of metastable phases (blue) (redrawn from [38]). Metastable phases which can be prepared by quenching to room temperature are indicated at the bottom. Note that the equilibrium m-t phase transition temperature is assumed to be much higher than in the general Zr-Y-O phase diagram (Figure 2.3). This is most likely due to the presence of metastable phases even for relatively slow temperature ramps.